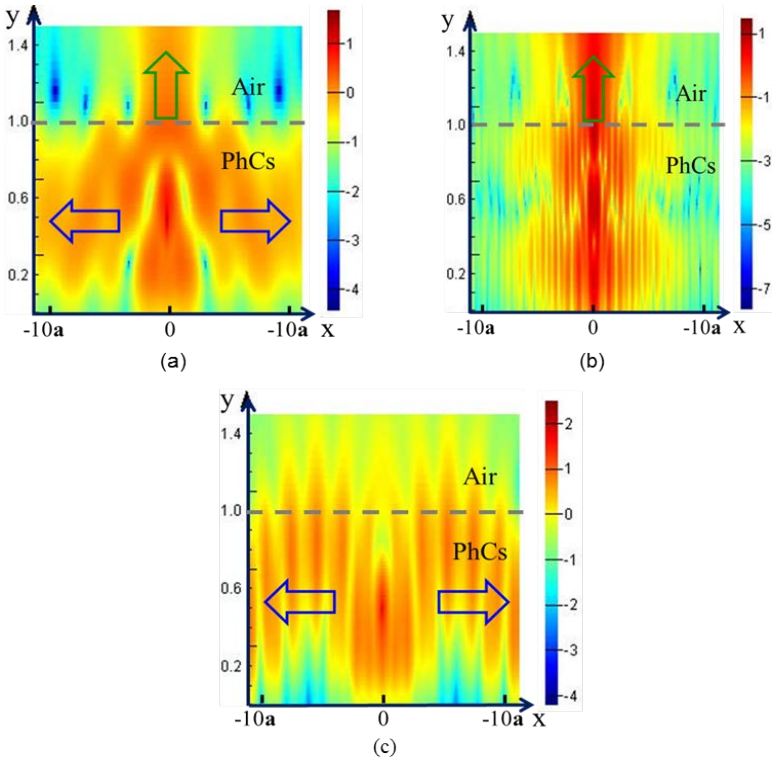

Fig. 4. The simulated patterns of PL emission at λ = 1530 nm (a) without PhC structure, (b) with **a** = 800 nm PhC array, and (c) with **a** = 300 nm PhC array. The film thickness is 1 um (From y = 0 to y = 1). The green arrows and the blue arrows indicate the surface emission and the waveguide propagation, respectively.

The PL emission patterns for different structures at λ = 1530 nm are displayed in Figs. 4(a)–4(c). Figure 4(a) shows the PL intensity profile of a film when there is no PhC array. The PL light from the center dipole is uniformly emitted in horizontal and vertical directions, and the PL fluxes passing through the top sensor and the side sensor are of the same order of magnitude. For the surface emission, a small cone of PL radiation is observed, whereas for the side emission, the PL propagates laterally inside the Er^{3+}-TeO_2 layer and the light wave bounces back and forth between two interfaces: air to Er^{3+}-TeO_2 film and Er^{3+}-TeO_2 film to Si wafer. For comparison, the PL intensity profile from a PhC array at **a** = 800 nm is shown in Fig. 4(b). A strong PL signal is observed at the top film surface where the PL light is projected upward to the air. Clearly, the PhC induces a highly anisotropic emission pattern; the surface PL is almost four orders of magnitude higher than lateral PL. The PL profile illustrates that the PhC array significantly enhances the extraction of the surface PL. On the other hand, Fig. 4(c) shows that the PhC with **a** = 300 nm has a highly confined waveguide mode; the PL intensity detected from the side sensor is four times higher than the intensity read by the top sensor. This indicates that most PL light remains in the Er^{3+}-TeO_2 film layer since surface PL extraction is strongly suppressed. As PhC periodicities decrease from **a** = 800 nm to **a** = 300 nm, the side PL signal is enhanced by four orders of magnitude. Figures 4(a)–4(c) document that the PL emission patterns from Er^{3+}-TeO_2 thin films can be readily manipulated by optimizing the structure of the PhCs, and switching between the surface emission mode and waveguide propagation mode is achieved by adjusting the PhC periodicity **a**.

Enhancement factors *F* at different PhC periodicities **a** are calculated and drawn in Fig. 5 in order to investigate the dependence of anisotropic PL emission on the PhC structures. In

#157346 - $15.00 USD Received 1 Nov 2011; revised 25 Dec 2011; accepted 6 Jan 2012; published 17 Jan 2012
(C) 2012 OSA

the equations below, F_S and F_W are the PL enhancement factors for the surface emission mode and the waveguide propagation mode respectively. They are defined as follows:

$$F_s = \frac{I_s - I_{sb}}{I_{sb}}$$

$$F_w = \frac{I_w - I_{wb}}{I_{wb}}$$

I_s is the PL intensity above the air – Er^{3+}-TeO_2 interface, where the light is extracted from the emission layer; I_w is the lateral PL signal observed at the edges of the Er^{3+}-TeO_2 film and refers to the PL in the waveguide planar mode. Both I_s and I_w are measured in the presence of a PhC array. I_{sb} and I_{wb} are the backgrounds PL signals for the two modes when no PhC structure exists. We find that surface PL enhancement factors F_S are positive when periodicity **a** is larger than 500 nm. A maximum F_S is observed for PhC with **a** = 800 nm while the waveguide PL enhancement factor F_W is negative when **a** is larger than 400 nm. Together the positive F_S and negative F_W indicate that surface emission is dominant, and the PL waveguide confinement is depressed. Therefore, the PhCs structure can efficiently extract PL light from Er^{3+}-TeO_2 layers into the air. In contrast, F_S becomes negative when **a**<500 nm while F_W becomes positive, and sharply increases from −50% to + 50% when **a** approaches 350 nm. The change of both factors, F_W (negative to positive) and F_S (positive to negative), reveals that most PL light is confined inside the Er^{3+}-TeO_2 layer appears in a waveguide propagation mode.

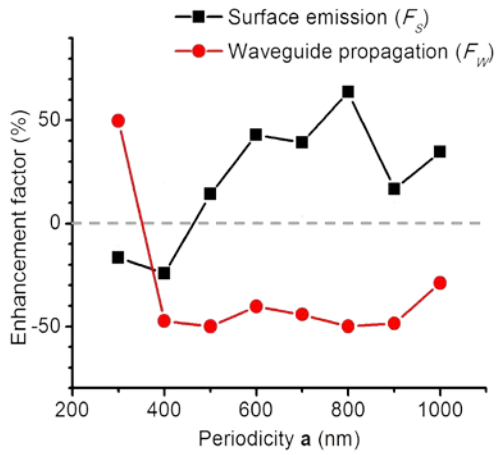

Fig. 5. Enhancement factors F_S and F_W simulated at different PhC periodicities **a**.

Note that the plot of F vs. **a** drawn from results of the simulation shows the same tendency as for the F vs. **a** plot shown in Fig. 3 (derived from experimental data). Both plots reveal that the critical PhC periodicity $\mathbf{a_C}$ triggers a mode transition. When **a** > $\mathbf{a_C}$, surface PL emission is preferred, and as the value of **a** decreases, F_S also gradually decreases while F_W remains negative. Once **a** reaches $\mathbf{a_C}$, F_S turns negative and F_W increases rapidly. This explains why the PL mapping shown in Fig. 2(b) exhibits destructive surface PL at **a** = 360 nm. Another tendency seen in the ***F*** vs. **a** plot is the existence of maximum F_S. Instead of monotonically increasing with the periodicity **a**, F_S reaches its highest value, 1.3, at **a** = 800 nm then decreases. These results correspond to the plot of measured F_S vs. **a** in Fig. 3 in which the maximum F_S value is observed between **a** = 800 nm and **a** = 1100 nm. Hence, the F vs. **a** relationship derived from FDTD simulation agrees well with the F_S vs. **a** variation observed experimentally. This varies that the anisotropic PL emission from Er^{3+}-TeO_2 PhCs can be accurately predicted by the simulation. Also, by modulating the percentage of PhC structures we can easily enhance the PL extraction ratio and determine the PL projection patterns.

#157346 - $15.00 USD Received 1 Nov 2011; revised 25 Dec 2011; accepted 6 Jan 2012; published 17 Jan 2012
(C) 2012 OSA

To explain the anisotropic emission, the photonic band structure of Er^{3+}-TeO_2 PhCs is calculated and shown in Fig. 6. From the diagram we find two photonic band gaps. The first gap is from 0.25f to 0.3f, where f is the normalized frequency equal to **a**/c Hz. The second gap is from 0.48f to 0.55f with a narrow band in the gap center. For a PhC with periodicity **a** = 800 nm, the second gap covers from λ = 1455 nm to 1667 nm. Clearly this band gap overlaps with the PL emission spectrum of Er^{3+}-TeO_2, and it prohibits the in-plane light propagation of emitted PL. Under this circumstance, only the surface emission mode exists and the enhancement factor of surface extraction F_S reaches its maximum at **a** = 800 as shown in Fig. 5. On the other hand, for PhCs at **a** = 300 nm PL at wavelength λ = 1530 nm has a normalized frequency f = 0.2. Since there is no band gap below f = 0.25, the PL light can easily couple into the thin film layer as the waveguide propagation mode. It explains the rapid increase of F_W when the periodicity **a** approaches 300 nm as shown in Fig. 5. Hence, the calculated band structure interprets the observed anisotropic patterns from PL emission and the transition of modes between the surface extraction and waveguide propagation.

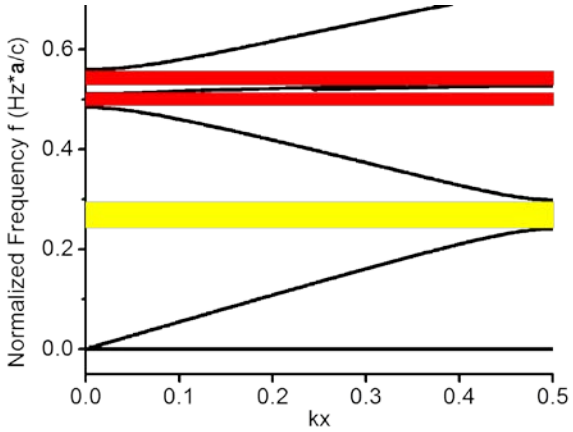

Fig. 6. Calculated photonic band diagram of Er^{3+}-TeO_2 PhCs. The yellow and red bars indicate the 1st and the 2nd photonic band gaps, respectively. kx is the wavevector in the Γ-X direction.

To investigate the broadband properties of PL enhancement, anisotropic emission enhancement factors F_S and F_W from λ = 1.50 μm to λ = 1.56 μm were analyzed. The PL intensities in the surface extraction mode and waveguide propagation modes were calculated by 2-D FDTD simulation. Figure 7(a) shows the spectral F_S and F_W values for PhCs with **a** = 800 nm. This value for **a** was chosen based on findings shown in Fig. 5 where a PhC with **a** = 800 nm had the highest surface emission ratio). As shown in Fig. 7(a), F_S is 80% at Δ = 1.50 μm, and it drops to 55% at Δ = 1.56 μm. Therefore, though F_S decreases as the wavelength of the PL increases, enhancement of surface emission beyond 50% is observed over the entire PL spectrum. Meanwhile F_W remains −50% over the entire PL spectrum implying that the planar waveguide mode PL has been suppressed. Therefore, we have demonstrated that the PhC with **a** = 800 nm can significantly improve the efficiency of broadband surface extraction.

#157346 - $15.00 USD Received 1 Nov 2011; revised 25 Dec 2011; accepted 6 Jan 2012; published 17 Jan 2012
(C) 2012 OSA

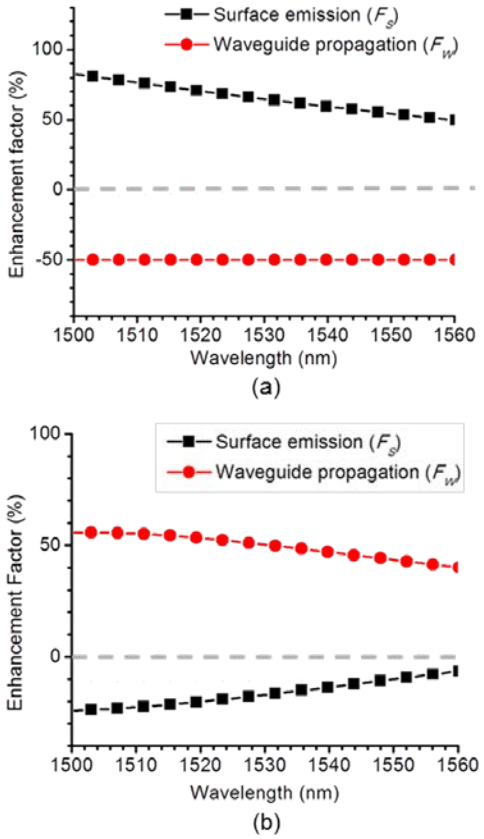

Fig. 7. Anisotropic emission enhancement factors F_S and F_W from λ = 1.50 μm to λ = 1.56 μm for PhCs with (a) **a** = 800 nm and (b) **a** = 300 nm.

Spectral enhancement factors for a PhC with **a** = 300 nm are also characterized and shown in Fig. 7(b) since this PhC demonstrates a strong waveguide propagation mode. The enhancement factor for the waveguide mode F_W is 55% at λ = 1.50 μm and slightly decreases to 45% at λ = 1.56 μm while surface emission enhancement F_S increases from –25% to –10% with an increase in PL wavelength. An averaged F_W of 50% is demonstrated in the overall PL spectra. By using PhCs with **a** = 300 nm, the broadband PL can be highly confined in the Er^{3+}-TeO_2 layer. Figure 7(a) and 7(b) thus document that the emission pattern can be spatially modulated according to the needs of the integrated photonic devices. PL enhancement exhibits a low variation as the emission wavelength changes. Broadband PL emission can be anisotropically projected into in-plane micro-cavities or adjacent layers with biochemical sensors.

4. Conclusion

In conclusion, we have demonstrated that Er^{3+}-TeO_2 thin films using PhC structures can serve as a broadband nano-optical coupler between two emission modes: the surface PL mission and waveguide PL propagation. By optimizing the PhC structure, 1500 nm-1560 nm broadband PL emission from Er^{3+}-TeO_2 is successfully converted between these anisotropic modes. 60% enhancement of surface extraction efficiency is achieved when PhC with periodicity **a** = 800 nm is applied. 85% enhancement is observed for waveguide PL emission, at **a** = 300 nm. The high level of flexibility of emission mode selection and the enhancement of broadband PL make Er^{3+}-TeO_2 PhCs thin films a potential light source for three dimensional integrated photonic circuits.

#157346 - $15.00 USD Received 1 Nov 2011; revised 25 Dec 2011; accepted 6 Jan 2012; published 17 Jan 2012
(C) 2012 OSA

Acknowledgments

The authors thank Lirong Z. Broderick and Xing Sheng for helpful discussions, and Kurt Broderick for his expert technical collaboration. This study was supported by a grant from Masdar Institute of Science and Technology (Abu Dhabi, UAE).

#157346 - $15.00 USD Received 1 Nov 2011; revised 25 Dec 2011; accepted 6 Jan 2012; published 17 Jan 2012
(C) 2012 OSA